

ACTIVITY ASSOCIATED WITH THE SOLAR ORIGIN OF CORONAL MASS EJECTIONS

D. F. WEBB*

American Science and Engineering, Inc., Cambridge, MA 02139, U.S.A.

and

Emmanuel College, Boston, MA 02115, U.S.A.

and

A. J. HUNDHAUSEN

*High Altitude Observatory, National Center for Atmospheric Research**, Boulder, CO 80307, U.S.A.*

(Received 24 September, 1986; in revised form 24 January, 1987)

Abstract. Solar coronal mass ejections (CMEs) observed in 1980 with the HAO Coronagraph/Polarimeter on the Solar Maximum Mission (SMM) satellite are compared with other forms of solar activity that might be physically related to the ejections. The solar phenomena checked and the method of association used were intentionally patterned after those of Munro *et al.*'s (1979) analysis of mass ejections observed with the Skylab coronagraph to facilitate comparison of the two epochs. Comparison of the results reveals that the types and degree of CME associations are similar near solar activity minimum and at maximum. For both epochs, most CMEs with associations had associated eruptive prominences and the proportions of association of all types of activity were similar. We also found a high percentage of association between SMM CMEs and X-ray long duration events (LDEs), in agreement with Skylab results. We conclude that most CMEs are the result of the destabilization and eruption of a prominence and its overlying coronal structure, or of a magnetic structure capable of supporting a prominence.

1. Introduction

The Skylab coronagraph observations established coronal mass ejections (CMEs) as an exciting and important aspect of the physics of the solar corona (see the reviews by Hildner, 1977; Rust *et al.*, 1980; and MacQueen, 1980). However, despite intensive study, the question of the physical and phenomenological origins of CMEs remains unanswered. One way to improve our understanding of the initiation of CMEs is to search for and assess the probability of their association with other kinds of solar activity that occur near the estimated CME onset time. Such studies during Skylab revealed a high percentage of association between CMEs and other chromospheric and coronal transient phenomena such as eruptive prominences, large flares, metric type II and IV radio bursts and X-ray long duration events (LDEs) (e.g., Munro *et al.*, 1979, hereafter Paper I, and Kahler, 1977). Of these phenomena, prominence eruptions and LDEs appear to be most clearly related to the origin of CMEs (Sheeley *et al.*, 1975; Webb *et al.*, 1976; Kahler, 1977; Pallavicini *et al.*, 1977). The associations of Skylab CMEs with

* Much of this work was performed as a Visiting Scientist at the High Altitude Observatory/NCAR.

** The National Center for Atmospheric Research is sponsored by the National Science Foundation.

eruptive prominences and LDEs were sufficiently high ($\geq 80\%$) to conclude that the phenomena were physically related. Subsequently, models were formulated that relate the origin of the CME to an erupting prominence and associated coronal heating (the LDE) via reconnection of magnetic fields (e.g., Anzer and Pneuman, 1982; Forbes and Priest, 1983). Other recent models (Low *et al.*, 1982; Wolfson, 1982) have ascribed the primary cause of some CMEs to the evolution to a non-equilibrium state of the large-scale magnetic structure over a prominence.

Recent observations of coronal mass ejections using both ground-based and spacecraft-borne coronagraphs have provided a large data base for the study of CMEs during and after the sunspot maximum of the present cycle. Studies based on data from coronagraphs on the SMM (Hundhausen *et al.*, 1984; Wagner, 1984; Hundhausen, 1987; Sawyer, private communication) and P-78 satellites (Poland *et al.*, 1981; Sheeley *et al.*, 1982; Howard *et al.*, 1985, 1986) indicate that some characteristics of CMEs, such as a nearly constant outward velocity above about $2 R_{\odot}$ and an average mass of several $\times 10^{15}$ g, remain essentially unchanged through a major part of the solar cycle. Other characteristics, such as their frequency of occurrence, heliolatitude distribution, and average velocity, have varied significantly since Skylab.

The purpose of our study is to assess the physical relationship between CMEs and other solar activity to better understand the origin or the initiation process of CMEs. Although our approach is mainly statistical, we feel that the results strongly support a close physical association between typical CMEs and erupting prominences. Our approach was to examine the associations between CMEs observed by the SMM coronagraph and other forms of solar activity during 1980, the epoch of sunspot maximum, and compare them with CME associations found for the Skylab-epoch (1973–1974) of declining sunspot activity by Munro *et al.* in Paper I. A complete tabulation of the 1980 SMM CME associations used in our study is available as an NCAR report (Webb, 1987). Preliminary studies of CME associations around sunspot maximum have revealed a similar pattern of associations to those obtained during the Skylab epoch (Poland *et al.*, 1981; Wagner, 1984, 1985; and Sawyer, private communication). And recently, Sheeley *et al.* (1983) showed that the degree of association between CMEs and X-ray events around solar maximum with durations > 4 hr was comparable to that during the Skylab epoch. We also examined the association of the SMM CMEs with X-ray LDEs observed with the NOAA GOES-2 satellite. Finally, we intercompared the different types of CME associations for both the Skylab and the SMM periods with respect to frequency of occurrence and heliolatitude distribution. We found an overall pattern of association similar to that of Paper I, but with some differences that probably reflect the different level of solar activity between the two epochs. We conclude that these results are most consistent with mass ejection models which feature prominence eruptions as a signature of magnetic control of the process.

In the next section we describe the data selection and association criteria. In Section 3 we discuss the overall results and the statistical significance of the associations between CMEs and other forms of solar activity, and in Section 4 we discuss the CME/X-ray LDE association study. Comparisons of the classes of CME associations with distribu-

tions of filaments, H-alpha flares and eruptive events and sunspot regions are made in Section 5, and in the last section the results are summarized and discussed.

2. Approach to the Study of Associations of CMEs with Other Solar Activity

2.1. DATA SELECTION

The HAO Coronagraph/Polarimeter on the SMM spacecraft was designed to observe temporal changes in the structure of the corona on time scales as short as tens of sec. The field of view of the coronagraph extended from 1.6 to 5 solar radii; see MacQueen *et al.* (1980) and Csoeke-Poeckh *et al.* (1982) for descriptions of the instrument and its operation. The coronagraph failed in late 1980 after imaging the corona over a 7-mo period. The instrument was repaired along with the SMM pointing system in April 1984 and has operated nearly continuously since then. This study concerns CME associations only for the 1980 epoch, which we hereafter designate as SMM I.

A CME is defined as a new, discrete brightening in the field of view over a time-scale of tens of minutes (Hundhausen *et al.*, 1984). These brightenings imply the addition of matter on this time-scale above the coronagraph's occulting disk. When a sequence of images is available, the discrete brightenings are always observed to move outward through the field of view, directly justifying their interpretation as mass ejections. The compilation of any list of CMEs involves subjective judgments, and in particular the establishment of some threshold of brightness and/or discreteness for the inclusion of events. Our procedure for the identification of CMEs is essentially the same as used during Skylab and, because of the similarity of the Skylab and SMM coronagraphs, should yield comparable lists of events for the Skylab (during sunspot decline) and SMM I (sunspot maximum) epochs.

A preliminary list of SMM I CMEs was compiled (Sawyer, private communication) by examination of film copies of all images and modified through re-examination by HAO SMM personnel of these images, each of which was examined digitally on an interactive video system. A total of 58 CMEs were sufficiently well observed to permit measurement of four properties used in this analysis: the apparent radial expansion speed, the estimated 'departure' or 'onset' time, the central axis position and the angular width. The radial speed of each CME was determined by following the visible edge of the outermost distinct bright feature on a time-sequence of direct coronagraph images and confirming the radial position of that edge. An uncertainty was assigned by examining a scan of the observed brightness vs heliocentric distance and performing a linear least-squares fit to the resulting plot of position vs time (with each point weighted inversely to the uncertainty in the position measurement). This procedure was carried out at several position angles near the central axis of the event to yield the radial velocity component and an estimate of its uncertainty based on the goodness of the linear least-squares fit and the reproducibility of the measurements at different angles. The uncertainty in these measurements varied from a few percent (for a few well-observed, bright events with sharp edges) to as much as 50% (for some poorly observed and many

slow-moving events), with an average uncertainty of $\sim 20\%$. The extrapolation of the linear least-squares fit inward to a heliocentric distance of $1 R_{\odot}$ yields the second property of interest, a departure time of the mass ejection from a presumed origin in the low corona or chromosphere. This time is, therefore, based on the assumption that the CME moved outward at constant velocity. The uncertainties in the departure time were again estimated from the goodness of the least-squares fit and the reproducibility of the results. These uncertainties ranged from 5 min to several hours in many slow events, with a mean uncertainty of ± 35 min.

Two additional properties, the central axis position and the angular width of the CME were determined by identification of the azimuthal position angles of the two sides of the bright feature. Confirmation of the angles and assignment of uncertainties was based on a scan of the observed brightness as a function of position angle at the lowest heliocentric distance where good measurements could be made (typically $2\text{--}2.5 R_{\odot}$). Typical uncertainties were a few degrees. The width was taken to be the maximum (for a time-sequence of images) difference between the two sides, and the center to be the average position of the two sides. All of these measured quantities are, of course, projections on the 'plane of the sky'.

This CME data set was then compared with lists of H-alpha prominence activity, H-alpha and soft X-ray flares, and metric radio bursts to determine associations. The selection of the types of solar activity to be compared and the method of their collection were intentionally patterned after the methods of Paper I to make the results comparable. Table I summarizes the types of data on chromospheric and coronal activity that were searched for possible CME associations.

The list of the types of *H-alpha prominence activity* considered was similar to that collected by Munro *et al.* with these exceptions: (1) H-alpha eruptives or mass ejection reported in notes accompanying the H-alpha flare lists in the *Solar-Geophysical Data Bulletins* (SGD) were added. The particular notes we used are defined in the table. (2) Sprays and eruptive prominences (EPs) listed in the SGD tables 'Mass Ejections from the Sun' were used. (3) The Mauna Loa Observatory prominence monitor film was examined for EPLs during 16 SMM CME intervals when this film was available. Although for our study we had these 'extra' data sets on prominence activity available to us, Munro *et al.* had the use of some data sets that were more complete than ours, such as comprehensive, daily logs of solar activity compiled by NOAA. Therefore, we believe that the solar-activity data sets compiled for the two studies were generally comparable. Finally, we note that the situation regarding the reporting of EPs has not improved since the Skylab era (see Paper I and Webb *et al.*, 1976) and, therefore, that the association of EPs with CMEs may be underestimated.

We compiled the list of *H-alpha flares* through a search of the SGD comprehensive flare reports. We treated subflares differently than did Munro *et al.* Although they included subflares in their Skylab associations, Munro *et al.* found that subflares were unlikely to be associated with CMEs unless accompanied by H-alpha ejection. Because subflares were so numerous during 1980 (sunspot maximum), the probability of the random association of subflares with CMEs was very high. On the other hand, we did

TABLE I
Data searched for CME associations

Data	Source
1. Prominence activity lists (EPL, DB or DSF, BSL, SPY) (Flare notes: A, H, L, S, U, Y) ^a	C. Sawyer (private communication) SGD Comprehensive Flare Reports WDC Observatory Logs of Active Prominences and Filaments SGD list of Mass Ejections J. Joselyn list of DSFs (private communications) B. Rompolt list of Active Prominences observed at Wroclaw Observatory (private communication) K. Rock <i>et al.</i> (1983)
MLO Prominence Monitor film	R. Fisher (private communication)
2. H-alpha flares	SGD Comprehensive Flare Reports
3. Soft X-ray events	NOAA GOES-2 plots provided by NOAA. SMM HXIS and XRP data (R. Harrison, private communication)
4. Metric continuum, type I, II, and IV radio bursts	Robinson <i>et al.</i> (1983) S. Kahler list (private communication) SGD Solar Radio Spectral Observations

^a A: Eruptive prominence with base less than 90° from central meridian.

H: Flare with high-speed dark filament.

L: Existing filaments show sudden activity.

S: Brightness follows disappearance of filament.

U: Two bright branches (two-ribbon flares).

Y: Loop prominence system.

not feel justified in totally eliminating subflares from consideration, because H-alpha flare importances can be underestimated near the limb and important coronal events can be accompanied by only minimal chromospheric brightening (e.g., Webb *et al.*, 1976). Therefore, a subflare was only considered associated with the CME (at moderate confidence) if it otherwise met the highest confidence criteria (see below) *and* if H-alpha-emitting ejecta accompanied the subflare. All other subflares were assigned low weight and not considered further in this analysis.

We compiled a list of *soft X-ray events* by examining GOES-2 6-hr, whole-Sun plots that were provided by NOAA to the SMM experimenters. LDEs and shorter-lived X-ray events were tabulated separately. Details of the X-ray/CME study are discussed in Section 4. Finally, we obtained lists of *metric radio bursts* during 1980 from these compilations: (1) the catalog of major metric bursts recorded at Culgoora, Australia (Robinson *et al.*, 1983), (2) a list culled from the SGD for the time period 1979–1982 (S. Kahler, private communication), and (3) the SGD table of ‘Solar Radio Spectral Observations’. Unlike Paper I, we searched for metric continuum and type I activity as well as type II and IV radio bursts, but tabulated their CME associations separately.

The metric continuum or type I associations were generally assigned low weight unless accompanied by flares or EP.

2.2. CRITERIA FOR ASSOCIATION

In contrast to Paper I, our study involved only the search for solar activity that could be associated with our list of CMEs, not the reverse. However, as in Paper I, we assigned to each association between a CME and a chromospheric or low coronal event a degree of confidence based on (1) the temporal separation between that activity and the estimated CME departure time and (2) the spatial separation of the two events. For each CME we used the uncertainty in that CME's departure time to define a variable time window for establishing associations. We believe the use of such a time window based solely upon the actual measurement of the CME trajectory to be more objective than the use of a relatively constant window as in Paper I. The need for a more sophisticated and objective time criterion was critical during 1980 when solar activity was high and, therefore, the probability of random association greater. However, for more direct comparison with Paper I, we repeated our analysis with a fixed time window centered on the estimated CME departure time. We defined a window of ± 90 min, which would have been long enough to encompass all but two of the Paper I associations. Any such choice of window duration represents a compromise between missing potentially important activity with uncertain onsets, and including increasingly spurious associations resulting from the use of a longer time window. 86% of the SMM associations fell within the ± 90 min window. The remaining associations arose from 9 CMEs for which the *variable* time window exceeded ± 90 min. These CMEs tended to be very slow, i.e., with speeds $\leq 100 \text{ km s}^{-1}$.

Our spatial association criteria were similar to Paper I. The *highest* confidence level of an association was assigned to an event whose onset occurred within the variable estimated CME departure time window (if less than ± 90 min), and the location of the event was within $\pm 20^\circ$ solar latitude* (or position angle) of the central radial axis of the CME and within 30° in solar longitude of the limb where the CME was observed. The second, or *moderate* confidence level, was assigned if one or more of these criteria were relaxed as follows: the event began during the fixed time window, or the variable window if longer than ± 90 min, and within $\pm 30^\circ$ latitude of the CME axis and 45° longitude of the limb.

The *lowest* confidence level was assigned if any one of the relaxed time and space criteria above were not met, or if the associated activity was an Active Prominence Region (APR), a Bright Surge at the Limb (BSL) of importance unspecified or 1, or an H-alpha subflare without ejecta. A few otherwise higher quality associated events had onsets after the time that the CME was first observed in the coronagraph field of view.

* One can argue that a more appropriate latitude window would vary according to the latitude limits of the actual CME structure. We also tabulated this value for each CME and found that in nearly every case the fixed $\pm 20^\circ$ latitude window encompassed the CME latitude band. Statistically this is understandable because most of the CME structures were $> 20^\circ$ wide (Hundhausen, 1987).

Since such events were unlikely to be associated with the onset of the CME, they were assigned low weight.

3. Results of the Associations

3.1. OVERALL RESULTS

Comparison of the 58 CMEs with speed measurements and the solar activity lists using the rigorous criteria yielded the following breakdown by confidence level of the highest rated associated activity within each CME time window: high = 12 CMEs, moderate = 26, low = 15, no association = 5. From now on we regard the associations at only the two highest levels to be significant. Therefore, 20 of the SMM CMEs were essentially unassociated, leaving 66% (38 of 58) of the CMEs likely or probably associated with the forms of solar activity we considered. This agrees reasonably well with Skylab where 78% (31 of 40) of the CMEs with speed measurements were considered to have 'definite' or 'probable' associations (Munro *et al.*, 1976)*. There were a total of 115 solar events associated with the SMM CMEs, or an average of about 2 apparent associations per CME. The Skylab ratio was about 1.6 associations per CME.

Table II summarizes these results in three 16-entry tables based on our comparisons between CMEs and the four categories of near-surface events that were candidates for CME association: erupting prominences, H-alpha flares, soft X-ray events, and type II and IV radio bursts. (Radio metric type I and continuum associated events are not included in these tables to facilitate comparison with the Skylab data.) Table IIA is for the SMM CME associations and Table IIB is for the Skylab CME associations. In these tables each of the CMEs will have one and only one entry whether or not it had multiple associations. For example, if we determined that CME 'X' was associated with two H-alpha flares, one EP and three radio bursts, a '1' would be entered in the box of the 'EP + HF' row and the 'RA' column. CMEs with no associations appear in the ('Neither . . . ; neither . . .') box. We made no correction for possible unobserved events arising from the invisible hemisphere ('backside') of the Sun. Paper I likewise made no correction for 'backside' events, but they estimated that perhaps half of the Skylab CMEs arose from such events.

Unlike the Skylab coronagraph, the SMM coronagraph contained an H-alpha filter which permitted the direct detection of neutral hydrogen material reaching the instrument's field of view, such as might be expected from a rising prominence. During 1980 we were able to confirm the existence of erupting prominence material in the outer corona through its detection with the coronagraph's H-alpha filter within the envelop of 8 CMEs. Most of the H-alpha-emitting features were highly structured bright regions,

* Paper I contains an inadequate discussion of how the Skylab associations were determined for CMEs with and without speed measurements. Although only 44% (34 of 77) of all of the Skylab CMEs had associations, the majority of the 43 CMEs without associations had no measured CME speed. So, in order to make the Skylab and SMM results comparable, we used the referenced 1976 HAO transient list to determine the percentage of associated Skylab CMEs.

TABLE II
Comparison between CMEs and four categories of near-surface events

	XR	XR + RA	RA	Neither XR nor RA	Total
A. SMM I CME associations					
EP	8	0	1	5	14
EP + HF	3	7	0	2	12
HF	1	1	0	0	2
Neither EP nor HF	7	2	1	20	30
Total	19	10	2	27	58
B. Skylab CME associations (from Paper I)					
EP	5	2	4	10	21
EP + HF	3	5	0	2	10
HF	0	1	2	0	3
Neither EP nor HF	0	0	0	43	43
Total	8	8	6	55	77
C. SMM I CME associations including CBRs as EPs and special cases					
EP	8	1	1	10	20
EP + HF	3	12	0	2	17
HF	0	1	0	0	1
Neither EP nor HF	6	2	1	13	22
Total	17	16	2	25	60

EP = Erupting prominences.

HF = H-alpha flares.

XR = Soft X-ray events.

RA = Radio metric type II, IV events.

and 6 of the 8 events were concentric with one or more outward-moving white light loops. Within 14 other CMEs (for a total of 21), similar highly structured central bright regions (CBRs) were detected but either were only observed in the broadband filter or were not emitting in H-alpha. Twenty of the 21 CMEs with CBRs had leading white light loops. We believe that all of these CBRs actually were EP remnants seen in the coronagraph field of view; indeed 15 of these 21 CMEs could be confidently associated with near-surface erupting or active H-alpha prominences.

However, to be conservative these CBRs were not used as evidence of the near-surface association of a CME with an EP. Therefore, they were excluded from Table IIA and our earlier statistical results. Also excluded were several associations for which detailed event studies have shown a likely association with a CME, but which did not meet our rigorous criteria for moderate or high confidence association. Because of their likely importance to the physical origin of CMEs, tabulating the CBRs as EPs and these special cases allows us to go a step further in our association study than Munro *et al.* Table IIC summarizes the results of including all SMM CME CBRs as EP associations

(whether or not they had associated ground-based H-alpha EPs) and the special cases in the study. Inclusion of these associations results in a higher proportion of associated CMEs and specifically, of EP-associated CMEs during SMM I.

TABLE III
Comparison of events associated with CMEs

Association type	Skylab		SMM I		SMM I ^a	
	No.	%	No.	%	No.	%
Erupting prominences	31	91	26	68	37	79
H-alpha flares	13	38	14	37	18	38
X-ray events	16	47	29	76	33	70
Radio II, IV events	14	41	12	32	18	38

^a Includes CBRs as EPs and special cases. The total number of associated CMEs are Skylab = 34, SMM I = 38, and SMM I^a = 47.

In Table III we have ordered the Skylab and SMM CME associations (Table II) by the total number of a given type of associated activity. The columns include CMEs with multiple associations, so, for example, the flare category lists the total number of H-alpha flares associated with CMEs whether or not the flares were associated with prominence eruptions, radio bursts or X-ray events. The percentage columns give the proportion of CMEs associated with the given activity type to the total number of CMEs *with associations*. In our tables we have defined erupting prominences to include *all eruptive activity* (including BSLs and sprays but not disk surges). We believe this is justified because Tandberg-Hanssen *et al.* (1980) showed that sprays should be considered merely fast filament eruptions. Paper I noted that 70% of the associated Skylab CMEs were associated with EPs or filament disappearances. Using our definition of EPs and Murno *et al.*'s activity list, we find that *nearly 90%* of the Skylab associations involved EPs, a slightly higher percentage than during SMM. Therefore, for both epochs *most* of those CMEs with associations had associated EPs. The percentages of CMEs associated with H-alpha flares and radio events were much lower and essentially unchanged between epochs, despite the greater activity rates near solar maximum.

To further clarify the role of EPs in the origin of CMEs, in Table IV we order the number of Skylab and SMM CMEs with a single association by the total number of the type of associated activity. 22 and 29% (with and without including CBRs and special cases) of all SMM I CMEs had single associations compared with 25% of Skylab CMEs. Note that for *both* Skylab and SMM there were *no* H-alpha flare-only CME associations! This table clearly reveals that EPs (and X-ray events) play an important role in the origin of CMEs.

Figure 1 shows the distribution of the offset time between the estimated CME departure and the onset of the associated activity for both SMM and Skylab (R. Munro, private communication). The offset time is plotted vs the number of associated events

TABLE IV
CMEs with single associations

Association type	Skylab	SMM I	SMM I ^a
Erupting prominences	10	5	10
H-alpha flares	0	0	0
X-ray events	0	7	6
Radio II, IV events	0	1	1
Total	10	13	17

^a Includes CBRs as EPs and special cases.

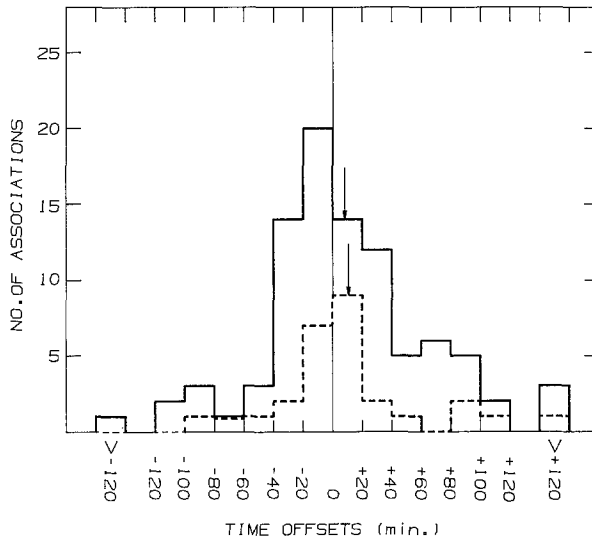


Fig. 1. The distribution of time offsets, in 20 min bins, between the estimated CME departure time and the onset time of the associated solar activity. A positive (negative) offset means the extrapolated CME onset lags (leads) the onset of the associated activity. The solid line is for SMM I (1980: 91 associated events) and the dashed line is for Skylab (1973–1974: 28 events). The arrows denote the algebraic averages of the offsets: SMM = +8.2 min; Skylab = +10.6 min.

in 20 min bins. The SMM distribution is broader than that for Skylab: slightly more than half of the Skylab associations began within 20 min of the CME departure time whereas for SMM half occurred within 30 min. The algebraic averages of the offsets for the two data sets are skewed in the positive sense (+11 and +8 min), meaning that on average the CME departure time lags the onset of its associated activity.

In principle, these offset times can be used to gain insight into the kinematics of CMEs. Using both K-coronameter and SMM coronagraph measurements of CMEs, MacQueen and Fisher (1983) concluded that EP-associated CMEs tend to have slower speeds but more significant accelerations through the lower corona than flare-associated

CMEs. In our study and that of Paper I, we assumed zero acceleration for each CME in estimating its departure time from the base of the corona. Significant acceleration of the CME below the coronagraph's occulting disk means that our estimated departure time will be too late. Also, if the disturbance actually forms well above the base of the corona, our time will be too late. Such a systematic shift might be detectable in an offset time plot and, indeed, the positive skew in the offset times of Figure 1 are consistent with a tendency for CME acceleration. The SMM height/time measurements reveal more direct evidence for significant acceleration within the coronagraph field of view for 30 of the 57 CMEs with measured speeds. In agreement with MacQueen and Fisher, most of these 30 CMEs were slower events associated with either EPs (16) or with no confident associations (9).

3.2. STATISTICAL SIGNIFICANCE OF THE ASSOCIATIONS

Munro *et al.* found that the probability that the association between the Skylab CMEs and the other forms of solar activity they checked were due to chance was exceedingly small. However, during the active part of the sunspot cycle we might expect the number of chance associations to be significantly higher. Therefore, it is necessary to confirm our expectation that the SMM associations we established were statistically significant and therefore that our association criteria were reasonable.

For this purpose we performed several significance tests on the data. We wanted to assess the probability of the random occurrence of the kinds of activity for which CME associations were sought within the time and spatial windows used for our association criteria.

We counted H-alpha flare and EP events over a 6-mo period from March through August 1980 (we did not consider X-ray or radio events for these tests). We used a compilation of all H-alpha flares provided by C. Sawyer (private communication). Because subflares dominate the flare population but are poorly correlated with CMEs, only flares of importance $\geq 1F$ were included in our sample. All H-alpha eruptive events with importances like those confidently associated with the CMEs; i.e., EPLs ≥ 1 , BSLs ≥ 2 , all sprays and all DBs or DSFs, were counted. Our CME association criteria required that the associated surface activity occur within $\pm 45^\circ$ of the limb and within $\pm 30^\circ$ latitude of the estimated launch position of the CME. Thus, if we assume that solar activity is equally likely to occur at any heliolongitude, then the spatial probability of occurrence can be approximated as $P_s = \Delta A/A \approx \frac{1}{4}$. (Although the latitude distribution of SMM CMEs was broader than that for Skylab, about $\frac{3}{4}$ of the SMM CMEs had their central axes at $\leq 45^\circ$ latitude.) The probability of occurrence of the events in time is approximately $P_t = \Delta t/T$, where Δt is the time window for the correlation of the CME and near-surface events and T is the total duration of the SMM observations. We used $\Delta t = 2$ hr, the average time window of our association criteria. The total probability of association will be

$$P = 1 - [(1 - P_t)P_s]^N,$$

where N is the total number of events observed over the period T . For these assumptions

$P = 0.24$. Since 28 of the CMEs had H-alpha flare and/or EP associations, we conclude that the probability that these associations were due to chance is extremely small.

Using more realistic estimates such as decreasing the spatial area, increasing the number of associated CMEs, or decreasing the number of chromospheric events (e.g., to assure that flares and EPs are independent of each other) all tend to decrease still further the probability of chance occurrence. Finally, in agreement with Paper I, we find that the temporal window for association would have to be opened to unrealistically long times (tens of hours) to permit the possibility of random occurrences affecting the degree of association. Therefore, we conclude that the SMM CME associations discussed in this paper are statistically significant and therefore that our criteria for association were reasonable.

4. The Association of SMM CMEs with X-Ray LDEs

The Skylab association among X-ray long-duration events (LDEs), CMEs and prominence eruptions was sufficiently high to conclude that these phenomena were physically related (Sheeley *et al.*, 1974; Webb *et al.*, 1976; Kahler, 1977; Pallavicini *et al.*, 1977). These studies used similar criteria to define and select LDEs for study. X-ray events having sufficiently shallow slopes during the decay portion of the flux vs time profiles and/or durations exceeding about 2 hr nearly always were associated with CMEs. Recently, Sheeley *et al.* (1983) have shown for a large sample of X-ray events and Solwind CMEs around solar cycle maximum that the proportion of the associated LDEs with CMEs is a smoothly increasing function of LDE duration from tens of min to hours with no short-lifetime cutoff. The percentage of association during the more active part of the cycle was similar to that during the Skylab epoch.

We have re-examined the strength of the association between LDEs and CMEs by using a sample of CMEs and LDEs obtained in conjunction with the general SMM CME association study (previous section). All soft X-ray events detected by the GOES-2 whole-Sun instrument which had their onset or peak time within the time windows described in Section 2.2 were listed. We made no judgment about the dependence of the association on the timing of the X-ray event within the window.

The 1–8 Å flux plots for the events in each window were used to determine the onset, peak and end times, decay duration (T_D) and exponential decay times (τ_d), the peak flux, whether the event was an LDE, whether it was associated with an H-alpha flare, and the likelihood of its association with the CME. T_D was defined as the duration from the time of the event peak to the time when the flux returned to the pre-event background. τ_d was defined as the time for the flux to decay to a level of $1/e$ of the peak, effectively the decay slope of the event.

During sunspot maximum the event decay duration (T_D) is not a useful way to identify LDEs in a whole-Sun detector like that on GOES because of the high background and the superposition of a large number of events. The higher background near solar maximum causes one to miss fainter events and to systematically underestimate event durations. The higher frequency of events results in fewer events with clean profiles and

a larger number of events for which only lower limits to the duration can be measured. For instance, in our sample lower limits only could be determined for about half of the measured events. To be consistent with the Skylab studies, we measured the exponential decay times (τ_d) of the events in an analogous way to Kahler (1977) and Pallavicini *et al.* (1977). Pallavicini *et al.* distinguished two classes of X-ray flares, one of which were LDEs which had longer decay durations, reached greater heights, had larger volumes and lower energy densities when compared with other flares. All of their LDEs had $\tau_d > 12$ min which we have adopted as the criterion for defining LDEs in our sample.

In most cases a listed H-alpha flare or eruptive event could be identified with an X-ray event, and the event's location could then be used to help determine the likelihood of its association with the given CME. For seven CMEs an X-ray event was the only associated solar activity; for these events only the timing could be used to determine the confidence of the association.

We summarized our results in the form of tables comparing the number of X-ray events within each fixed 3-hr CME window that were or were not associated with the CME against the number of these X-ray events that were or were not LDEs. There were total of 189 X-ray events occurring within the 58 CME time windows. Forty-one of the 189 X-ray events were likely associated with the CME. Twenty (49%) of these 41 CME-associated X-ray events were likely LDEs, 4 were questionable and 17 (41%) were short-lived events. To more clearly delineate physical associations, we also tabulated the distributions of only the single X-ray event in each window most likely to have been associated with the CME. Of 33 such X-ray events that were associated with a CME, 19 (58%) were likely LDEs, 3 were questionable, and 11 (33%) were short-lived events. This latter proportion of association is higher than Kahler (1977) found; only 9% (2 of 22) of the Skylab short-lived events $\geq 50\%$ from central meridian were associated with CMEs.

All of the short-lived CME/X-ray events for which slopes could be measured had $\tau_d < 10$ min, whereas the shortest CME/LDE event had $\tau_d = 15$ min. The distribution of SMM LDE decay times compared favorably with that of Skylab (Kahler, 1977). The SMM-I period occurred in the middle of the 3-yr interval which Sheeley *et al.* (1983) chose for their Solwind CME/LDE study. Although our sample was smaller than theirs, the durations (T_D) of the SMM CME/X-ray events tended to group in the ≤ 2 hr time interval, confirming Sheeley *et al.*'s result that shorter-duration X-ray events can be associated with CMEs. The proportion of LDEs associated with SMM CMEs (about 60%) was similar to Sheeley *et al.*'s results for CMEs with LDEs of duration $\gtrsim 3$ hr, and less than during Skylab. However, we believe the SMM results to be in reasonable agreement with the Skylab results, because the number of LDEs detected during SMM is probably an underestimate (because of the high background and frequency of events) and the decay times of CME/LDEs are equivalent. Therefore, we conclude that the percentage of association of LDEs with CMEs and the typical lifetimes of associated LDEs have not changed significantly between the decline of the last solar cycle and the peak of the present cycle. We emphasize that, like our other associations, the CME/LDE study was done only one way; we did not examine the

inverse correlation of CMEs for a given list of LDEs. Sheeley *et al.* (1983) found a similar percentage of association when the study was done in either direction.

Finally, we compared several characteristics and associations of the 19 probable CME/LDEs and the 11 CME/short-lived X-ray events to check for anything that might clearly distinguish the two X-ray classes. Our results are summarized in Table V. We have discussed the decay times, which we used to separate the classes. The two classes showed no significant differences in terms of the X-ray fluxes, the speed and latitude of the associated CME, the H-alpha longitude distribution, or the associations with metric events, H-alpha flares or EPs. Most of the short-lived events could be identified with specific active regions, whereas less than half of the LDEs could.

TABLE V
X-ray events associated with CMEs: characteristics and associations

Characteristics	Long-decay	Short-decay
X-ray decay time (τ_d -min): average/range	86/15–300	6.3/5–7
X-ray peak flux: average/range	M1.0/C1.3–M4	M1.5/C1.5–M7
CME speed (km s ⁻¹): average/range	382/24–1200	356/24–585
CME latitude: average/range	S12/S64–N47	S10/S56–N32
H-alpha longitude ^a :	3/3/2/10	0/2/5/4
< 45°/45–60°/60–75°/75–90°	12 of 17 > 60°	9 of 11 > 60°
Associations		
Identified with AR? (Y/?/N)	7/4/8	9/1/1
II and/or IV	7 of 19 (37%)	5 of 10 (50%)
Prominence eruptions	13 of 19 (68%)	6 of 10 (60%)
H-alpha flares (and HF + EP)	8 of 19 (42%)	5 of 10 (50%)

^a Distance from central meridian.

5. Solar Cycle Variations of CMEs and their Associations

If physically important for the origin of CMEs, a class of solar phenomenon purported to be associated with CMEs should exhibit long-term variations like those of the CMEs. Here we compare during the Skylab and SMM I epochs the frequency of occurrence and heliolatitude distributions of CMEs and their association classes, and H-alpha filaments and sunspot regions, and H-alpha flares and EPs. (A full statistical study of the solar cycle distributions of CME properties has recently been performed by Hundhausen (1987).)

Hundhausen *et al.* (1984) showed that there was only a 20% increase in the frequency of occurrence of CMEs between 1973 (Skylab) and 1980 (SMM I)*. Between equivalent

* There is some controversy over CME rates, due primarily to the higher rates derived from the Solwind coronagraph during the solar maximum period (e.g., Howard *et al.*, 1985, 1986; Hundhausen, 1987).

periods in 1973–1974 and 1980, we determined that the frequency of occurrence of sunspot groups, H-alpha flares, and metric type II bursts associated with flares increased by factors of 2.2, 4, and 5, respectively. The apparent high correlation between prominence activity and CMEs suggests that comparisons of CME characteristics with counts of filaments and filament eruptions should be fruitful. We used counts of all disk filaments provided by C. Hyder and E. Hildner (private communication) and found that the number of filaments had increased between Skylab and SMM I by a factor of only 1.5. (We reserve for a future paper a comparison of the rates of EPs during Skylab and SMM.)

The heliolatitude distributions of CMEs observed from Skylab and SMM I have been compared by Hundhausen *et al.* (1984) and Hundhausen (1987). Figure 2 presents revised distributions of these data in the form of stacked histograms for Skylab and SMM I of the heliolatitude distributions of the central axes of all CMEs (top), all disk filaments (Hyder and Hildner, private communication), all EPs (1980 only), and all sunspot groups (Hyder and Hildner). The distribution of all H-alpha flares was not determined but should closely resemble the sunspot distribution. During solar maximum CMEs were more uniformly distributed than during the Skylab epoch, with more events at high latitudes. The distribution of disk filaments (and EPs in 1980) was similar to that of the CMEs, including in 1980 the correspondence of a marked north–south asymmetry. To the contrary, the sunspot distributions showed sharp cutoffs above 20° for 1973 and 30° in 1980.

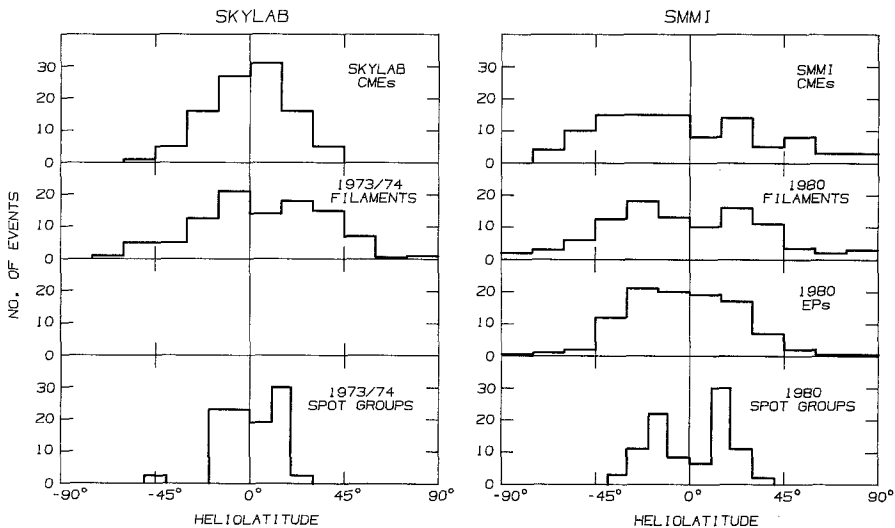


Fig. 2. Helio-latitude distributions of the central axes of all CMEs (top), all disk filaments, all erupting prominences, and all sunspot groups (bottom) during the Skylab (left) and SMM I (right) epochs. The distribution of EPs during Skylab was not determined. The sunspot distribution is plotted in 10° latitude bins, all others in 15° bins. Southern (northern) hemisphere data is to the left (right). The data sources were: Skylab CMEs: Hundhausen *et al.* (1984), disk filaments and sunspot groups: Hyder and Hildner (private communication), SMM CMEs and EPs: this work.

We conclude that at both epochs of the solar cycle, both the frequency of occurrence and latitude distribution of CMEs more closely matched that of EP-producing regions on the Sun (filaments) than of flare-producing regions (active regions).

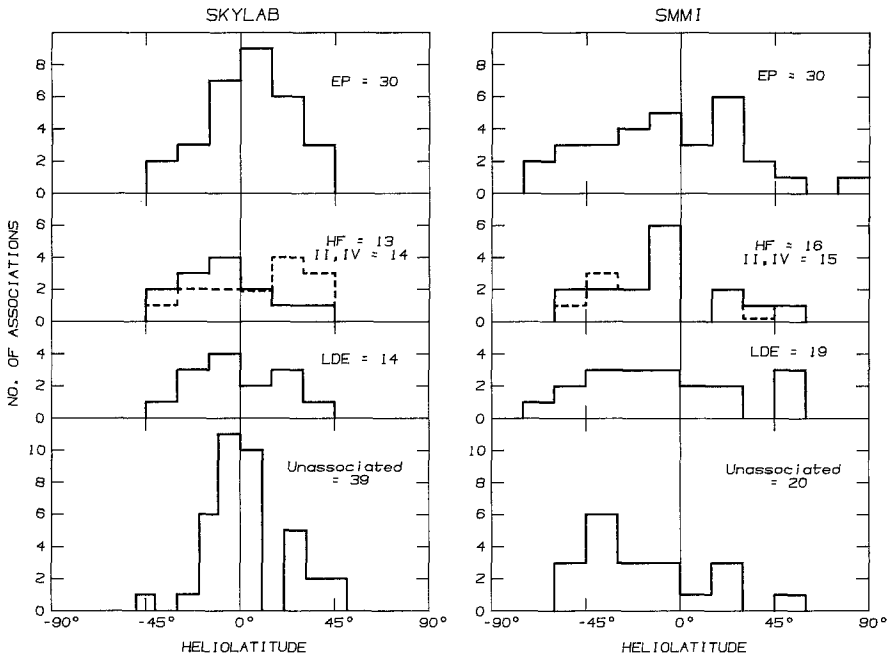


Fig. 3. Heliolatitude distributions of Skylab (*left*) and SMM I (*right*) CMEs by class of associated activity: EPs (*top*), H-alpha flares (*solid*) and metric type II, IV bursts (*dashed*), X-ray LDEs, and unassociated (*bottom*). Compare with Figure 2. The total number of CMEs in each class is shown in each panel. Because of multiple associations, a given CME can be represented in more than one association class. The Skylab data are from Paper I except for the 'unassociated' data, which are from Wagner 1984, 1985).

In Figure 3 we present histograms of the heliolatitude distributions of CMEs by the class of associated activity for Skylab and SMM I. For SMM I the distribution of EP-associated CMEs closely followed that of the 1980 disk filaments and EPs (Figure 2). For Skylab the CME/EP distribution peaked at the equator, in contrast to the broader distribution of 1973–1974 disk filaments (Figure 2), implying that a stronger active region component might have been involved in the origin of Skylab CMEs (e.g., Hildner, 1977). Finally, we confirm Wagner's (1984) observation that the latitude distribution of CMEs without good associations was quite different between 1973–1974 and 1980. Such Skylab CMEs were launched from a narrow zone within about $\pm 20^\circ$ of the equator, whereas the SMM distribution was broader with most such CMEs in the southern hemisphere.

6. Summary and Discussion

The overall goal of our study was to better understand the origins of CMEs. To this end we compared CMEs observed during 1980 with the SMM coronagraph with other types of solar activity to determine associations. We intentionally patterned our criteria for the selection of the types of solar activity to be considered and for the associations with CMEs after those used by Munro *et al.* (1979) in their study of Skylab CME associations to facilitate comparison of the two epochs, which were quite different in terms of solar activity.

We found associations for 66% of the SMM CMEs, a slightly lower rate than the 78% found for Skylab CMEs. For both epochs most CMEs with associations had associated prominence eruptions. In terms of CMEs with a single association, prominence eruptions and X-ray events were the dominant associations. This high proportion of association of CMEs with EP might actually be underestimated because eruptive events are underreported with respect to flares. The percentages of association of CMEs with H-alpha flares and type II or IV radio bursts were much lower than with EPs and similar for the Skylab and SMM periods. We found that about 60% of the GOES X-ray events associated with CMEs could be classified as LDEs, confirming previous results of a strong association between CMEs and LDEs (e.g., Kahler, 1977; Sheeley *et al.*, 1983).

For the sunspot maximum epoch, our results support the strong association discovered during Skylab between mass ejections observed in the outer corona and prominences erupting from near the solar surface. This conclusion is reinforced by comparison during Skylab and SMM I of the frequency of occurrence and heliolatitude distribution of CMEs, which more closely matched those of filaments in general rather than of H-alpha flares or active regions. And, especially in 1980, the latitude distribution of EPs closely matched that of the CMEs, including a distinct north-south asymmetry. Also, the existence of erupting prominence material at the core of CMEs was confirmed through the direct detection of its H-alpha emission with the SMM coronagraph. Similar bright central cores were discovered for one-third of the SMM I CMEs and for about 20% of all Skylab CMEs (Hildner, private communication). We consider these bright, structured cores to be actual prominence remnants, whether fully ionized or not, detected in the outer corona. Prominence ejecta have also been detected out to at least $9 R_{\odot}$ by the Solwind coronagraph.

In agreement with MacQueen and Fisher (1983), we found that the majority of SMM CMEs showed evidence of significant acceleration, and that most of these had slower speeds and were associated either with EPs or had no good association. However, we did not find the clean separation in kinematical behavior between EP-associated and flare-associated CMEs reported by MacQueen and Fisher in their study, which included observations in the low corona. They found that EP-associated CMEs tended to have slower speeds but more significant accelerations than flare-associated CMEs. The SMM measurements, all made above $1.6 R_{\odot}$, revealed *no* difference between the classes of flare-associated and *EP-only* associated CMEs in

terms of either their speeds or evidence of acceleration. The dominance of EP-associations makes such a comparison difficult, because in both our data and that of MacQueen and Fisher, there were few if any flare-only associations.

Finally, Wagner (1984, 1985) has suggested that the unassociated Skylab and SMM CMEs represent a class of 'spontaneous' mass ejections with unique characteristics. Our results reveal that the only distinctive characteristic of such CMEs is a tendency to have slower speeds. Slow CMEs tend to be fainter and their speeds harder to measure, and can also exhibit significant acceleration. Therefore, they are more likely to be associated with smaller, less detectable solar activity and to have a larger uncertainty in T_0 , the estimated CME onset time (MacQueen, 1985). Finally, contrary to Wagner's interpretation, we believe that the percentage of CMEs without good associations is similar and relatively low for both Skylab (Munro *et al.*, 1976) and SMM I, and consistent with their slow speeds and a contribution from undetected 'backside' activity. Therefore, we find no support for Wagner's interpretation of unassociated CMEs as a separate physical class.

Webb (1986) has described a phenomenological picture of the origin of mass ejections which organizes the essential observations in terms of a magnetic reconnection model (e.g., Anzer and Pneuman, 1982). Such models best match observations of double-ribbon H-alpha events with EPs, post-flare loops, X-ray and white light density depletions and white light 'disconnections'. In general, models featuring magnetic control of CMEs appear more compatible with the observations of especially the early phase of CMEs than compressional wave models. However, none of the models clearly address the actual cause of the destabilization of the filament and most of them are mathematically incomplete. We believe that future theoretical development of such models must incorporate realistic magnetic topologies and time-dependent magnetic restructuring of the corona.

Sufficient studies have now been made of the solar activity associated with the onset of CMEs to realize that the destabilization and eruption of prominences, or more generally of the magnetic structures within which prominences form, are responsible for *most*, if not all, mass ejections. This realization clearly has significant implications, not only for modeling of the early stage of CMEs, but also for the interplanetary consequences of such large-scale magnetic and plasma ejections.

Acknowledgements

One of the authors (DFW) expresses his gratitude for the support and guidance of the SMM C/P group at the High Altitude Observatory of NCAR where he was a visiting scientist during 1983 and 1985. We acknowledge helpful discussions with and contributions of data from R. Munro, W. Wagner, C. Sawyer, R. Fisher, R. MacQueen, R. Illing, D. Sime, E. Hildner, and S. Kahler. We appreciate the hard work and dedication of Joan Burkepille and Peter Reppert of HAO in the reduction and measurements of the digitized CME imagery. The National Center for Atmospheric Research is sponsored by the National Science Foundation. DFW's work on this study was

supported at AS&E by NASA under contracts NAS5-25496 and NAS5-28727 and at Emmanuel College by AFGL contract AF 19628-82-K-0039.

References

- Anzer, U. and Pneuman, G. W.: 1982, *Solar Phys.* **79**, 129.
- Csoeke-Poeckh, A., Lee, R. H., Wagner, W. J., House, L. L., Hildner, E., and Sawyer, C.: 1982, *J. Spacecraft* **19**, 345.
- Forbes, T. G. and Priest, E. R.: 1983, *Solar Phys.* **84**, 169.
- Hildner, E.: 1977, in M. A. Shea *et al.* (eds.), *Study of Travelling Interplanetary Phenomena*, D. Reidel Publ. Co., Dordrecht, Holland, p. 3.
- Howard, R. A., Sheeley, N. R., Jr., Koomen, M. J., and Michels, D. J.: 1985, *J. Geophys. Res.* **90**, 8173.
- Howard, R. A., Sheeley, N. R., Jr., Koomen, M. J., and Michels, D. J.: 1986, in R. G. Marsden (ed.), *The Sun and the Heliosphere in Three Dimensions*, D. Reidel Publ. Co., Dordrecht, Holland, p. 107.
- Hundhausen, A. J.: 1987, *J. Geophys. Res.* (submitted).
- Hundhausen, A. J., Sawyer, C. S., House, L., Illing, R. M. E., and Wagner, W. J.: 1984, *J. Geophys. Res.* **89**, 2639.
- Kahler, S.: 1977, *Astrophys. J.* **214**, 891.
- Low, B. C., Munro, R. H., and Fisher, R. R.: 1982, *Astrophys. J.* **254**, 335.
- MacQueen, R. M.: 1980, *Phil. Trans. R. Soc. London* **297**, 605.
- MacQueen, R. M.: 1985, *Solar Phys.* **95**, 359.
- MacQueen, R. M. and Fisher, R. R.: 1983, *Solar Phys.* **89**, 89.
- MacQueen, R. M., Csoeke-Poeckh, A., Hildner, E., House, L., Reynolds, R., Stanger, A., TePoel, H., and Wagner, W.: 1980, *Solar Phys.* **65**, 91.
- Munro, R., Hildner, E. and Roach, G.: 1976, 'Revised Transient List (as of 15 June 1976)' (unpublished).
- Munro, R. H., Gosling, J. T., Hildner, E., MacQueen, R. M., Poland, A. E., and Ross, C. L.: 1979, *Solar Phys.* **61**, 201.
- Pallavicini, R., Serio, S., and Vaiana, G. S.: 1977, *Astrophys. J.* **216**, 108.
- Poland, A. I., Howard, R. A., Koomen, M. J., Michels, D. J., and Sheeley, N. R., Jr.: 1981, *Solar Phys.* **69**, 169.
- Robinson, R. D., Tuxford, J. M., Sheridan, K. V., and Stewart, R. T.: 1983, *Proc. Astron. Soc. Aust.* **5**, 84.
- Rock, K., Fisher, R., Garcia, C., and Yasukawa, E.: 1983, *A Summary of Solar Activity Observed at the Mauna Loa Solar Observatory: 1980-1983*, NCAR TN-221, Boulder, CO.
- Rust, D. M., Hildner, E. and 11 co-authors: 1980, in P. Sturrock (ed.), *Solar Flares*, Colorado Assoc. Univ. Press, Boulder, CO, p. 273.
- Sheeley, N. R., Jr., and 12 co-authors: 1975, *Solar Phys.* **45**, 377.
- Sheeley, N. R., Jr., Howard, R. A., Koomen, M. J., Michels, D. J., Harvey, K. L., and Harvey, J. W.: 1982, *Space Sci. Rev.* **33**, 219.
- Sheeley, N. R., Jr., Howard, R. A., Koomen, M. J., and Michels, D. J.: 1983, *Astrophys. J.* **272**, 349.
- Tandberg-Hanssen, E., Martin, S. A., and Hansen, R. T.: 1980, *Solar Phys.* **65**, 357.
- Wagner, W. J.: 1984, *Ann. Rev. Astron. Astrophys.* **22**, 267.
- Wagner, W. J.: 1985, in C. de Jager and C. Biao (eds.), *Proc. of Kunming Workshop on Solar Physics and Interplanetary Travelling Phenomena*, Vol. 2, Science Press, Beijing, China, p. 969.
- Webb, D. F.: 1986, in M. R. Kundu *et al.* (eds.), *Solar Terrestrial Physics: Proc. of Second Indo-US Workshop on Solar-Terrestrial Physics*, Nat. Physical Lab, New Delhi, India, p. 283.
- Webb, D. F.: 1987, 'SMM I (1980) List of CME Associations', NCAR Technical Report (to be published).
- Webb, D. F., Krieger, A. S., and Rust, D. M.: 1976, *Solar Phys.* **48**, 159.
- Wolfson, R. L. T.: 1982, *Astrophys. J.* **255**, 774.